

# THERMOCYCLIC- AND STATIC-FAILURE CRITERIA FOR SINGLE-CRYSTAL SUPERALLOYS OF GAS-TURBINE BLADES

## TERMOCIKLIČNA IN STATIČNA MERILA ZA PORUŠITVE LOPATIC PLINSKIH TURBIN IZ MONOKRISTALNIH SUPERZLITIN

Leonid B. Getsov<sup>1</sup>, Artem S. Semenov<sup>2</sup>, Elena A. Tikhomirova<sup>3</sup>, Alexander I. Rybnikov<sup>1</sup>

<sup>1</sup>NPO ZKTI, Russia

<sup>2</sup>St. Petersburg State Polytechnical University, Russia

<sup>3</sup>Klimov Company, Russia

guetsov@yahoo.com, semenov.artem@googlemail.com

*Prejem rokopisa – received: 2013-05-17; sprejem za objavo – accepted for publication: 2013-06-28*

The problem of the thermo-mechanical fatigue (TMF) of single-crystal turbine blades has not been fully investigated theoretically or experimentally. In the present work TMF tests were performed for two single-crystal nickel-based alloys (ZhS36 and ZhS32) with various crystallographic orientations ( $\langle 001 \rangle$ ,  $\langle 011 \rangle$ ,  $\langle 111 \rangle$ ) under different temperatures and cycle durations. The dependence of the failure modes (crystallographic or non-crystallographic) on the loading regimes was analyzed. The non-linear viscoelastic, elastoplastic and viscoelastoplastic material models with non-linear kinematic hardening were used to predict the cyclic stress-strain state, ratcheting and creep of the samples. The deformation criterion of damage accumulation was introduced to the lifetime prediction. A stress analysis of the single-crystal samples, with concentrators (in the form of circular holes) and without them, was carried out using physical models of the plasticity and creep. These material models take into account that an inelastic deformation occurs due to a slip mechanism and it is determined with the crystallographic orientation. The proposed failure model using the deformation criterion allows qualitative and quantitative predictions of the TMF fracture process in single crystals.

Keywords: gas-turbine blade, single crystal, thermo-mechanical fatigue, damage, crystallographic and non-crystallographic failure modes

Problem termo-mehanske utrujenosti (TMF) monokristalnih turbinskih lopatic še ni v celoti raziskan niti teoretično niti eksperimentalno. V tem delu so bili izvršeni TMF-preizkusi na dveh monokristalnih zlitinah na osnovi niklja (ZhS36 in ZhS32) z različno kristalografsko orientacijo ( $\langle 001 \rangle$ ,  $\langle 011 \rangle$ ,  $\langle 111 \rangle$ ) pri različnih temperaturah in trajanju ciklov. Analizirana je bila odvisnost načina porušitve (kristalografska ali nekristalografska) od vrste obremenjevanja. Modeli nelinearne viskoelastičnosti, elastoplastičnosti in viskoelastoplastičnosti z nelinearnim kinematičnim utrjevanjem so bili uporabljeni za napovedovanje cikličnega stanja napetost – raztezek, nazobčanja in lezenja vzorcev. V napovedovanje dobe trajanja je bilo vpeljeno deformacijsko merilo akumuliranja poškodb. Izvršena je bila analiza napetosti v monokristalnem vzorcu s koncentraciji (v obliki okroglih lukenj) in brez njih, z uporabo fizikalnega modela plastičnosti in lezenja. Ti materialni modeli upoštevajo, da se pojavi neelastična deformacija z mehanizmom lezenja in je določena s kristalografsko orientacijo. Predlagani model porušitve z uporabo deformacijskih meril omogoča kvalitativno in kvantitativno napovedovanje TMF- procesa preloma monokristala.

Ključne besede: lopatica plinske turbine, monokristal, termo-mehanska utrujenost, poškodba, kristalografski in nekristalografski način porušitve

## 1 INTRODUCTION

The use of single-crystal alloys for the manufacturing of the blades of a gas-turbine engine allows a significant increase in the gas temperature before a turbine and sets a number of tasks that should help increase the reliability of a stress and strength analysis. In the present investigation, the results of the experimental studies of single-crystal nickel-based alloys, as well as the approaches to the computation of the stress-strain state and strength of the structural parts are considered and discussed.

## 2 MATERIALS AND METHODS OF RESEARCH

Numerous experimental studies were performed on two single-crystal alloys, ZhS32 and ZhS36 (Table 1) with different alloying and, most importantly, different

carbon amounts and were designed to expand the information given in<sup>1,2</sup>. The tests of the mechanical properties, creep and thermal-fatigue resistance at different temperatures were carried out.

The creep tests were conducted on an installation of ATS (Applied Test Systems, Inc.) determining the kinetics of the accumulated inelastic deformation during the first stage and in the steady state of the creep. The test methods for TMF are described in detail in<sup>3,4</sup>. For the tests, rigidly clamped samples with polished surfaces were used, as shown in Figure 1. The tests were conducted in a vacuum that allowed us, during the testing, to observe the formation of slip bands and crack initiation, and to determine the rate of the crack propagation on a polished surface using the magnification of 250-times.

The tests were conducted with various values for the maximum ( $T_{\max} = 900\text{--}1100\text{ }^{\circ}\text{C}$ ) and minimum ( $T_{\min} =$

**Table 1:** Chemical compositions of the ZhS32 and ZhS36 single-crystal alloys, w/%

**Tabela 1:** Kemijska sestava monokristalnih zlitin ZhS32 in ZhS36, w/%

Alloy	C	Cr	Co	Mo	W	Ta	Re	Nb	Al	Ti	Ni
ZhS32	0.12–0.18	4.3–5.6	8.0–10.0	0.8–1.4	7.7–9.5	3.5–4.5	3.5–4.5	1.4–1.8	5.6–6.3	–	Base
ZhS36	0.03	4.03	8.48	1.41	11.50	-	1.94	1.07	5.70	0.91	Base

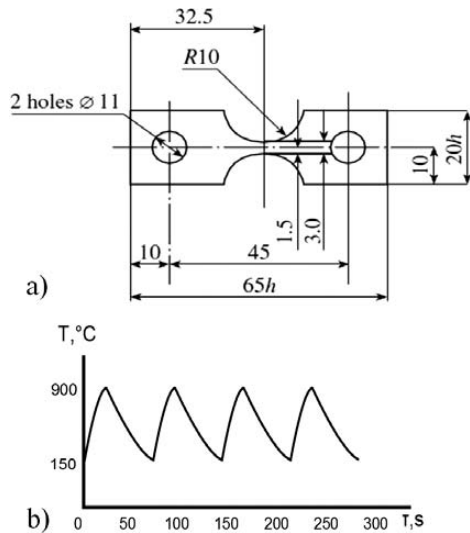


**Figure 1:** a) Specimen for the thermal-fatigue test, b) with typical cyclic-temperature changes over time in the central point

**Slika 1:** a) Vzorec za preizkus toplotnega utrujanja, b) z značilnim nihanjem temperature v srednjem delu

150–700 °C) cycle temperatures. The tests with the retardation times of 2 min and 5 min at  $T_{max}$  were carried out for some parts of the samples. Some samples had the stress concentrator in the form of a central hole with the diameter of 0.5 mm. The test specimens had different crystallographic orientations:  $\langle 001 \rangle$ ,  $\langle 011 \rangle$  or  $\langle 111 \rangle$ . To determine the crystallographic orientation for each sample Laue’s diffraction patterns were obtained and three Euler angles and Schmid factors were computed.

On the basis of the results of a crystallographic analysis, possible directions (angles) of the slip bands on the specimen surfaces were calculated with the aim to compare them with the angles, at which the samples

were destroyed. The location of the fracture nucleus was determined with the results of fractographic studies using a TESCAN microscope. The comparison of the experimental data on the orientation of the fracture surfaces with the results of the crystallographic analysis and with the results of the finite-element analysis of the specimens allowed us to define the dependence of the failure mechanism (crystallographic or non-crystallographic) on the parameters of the thermal cycle.

### 3 RESULTS OF EXPERIMENTAL STUDIES

The tests of mechanical properties show that single-crystal alloys do not have a high plasticity at all the temperatures (see, for example, **Table 2**). Low values of plasticity  $\delta$  are observed for the carbon-free ZhS36 alloy (as opposed to the carbon ZhS32 alloy) at 500 °C (as opposed to the cases of high temperatures where  $T > 900$  °C).

**Table 2:** Mechanical properties of single-crystal alloys with orientation  $\langle 001 \rangle$  at 500 °C

**Tabela 2:** Mehanske lastnosti monokristalne zlitine z orientacijo  $\langle 001 \rangle$  pri 500 °C

Alloy	$R_{p0.2}$ MPa	$R_m$ MPa	A %	Z %	
ZhS36	964	982	1.3	5.0	
	967	1000	2.3	6.9	
ZhS32	Schedule t/t 1	850	880	19.5	35.5
	Schedule t/t 2	810	1110	13.0	11.7

**Figure 2** shows the short-term creep curves of alloy ZhS32. The curves obtained under the stress of 550 MPa at 850 °C significantly differ for various samples. The results of the creep tests for alloy ZhS36 are given in<sup>5</sup>.

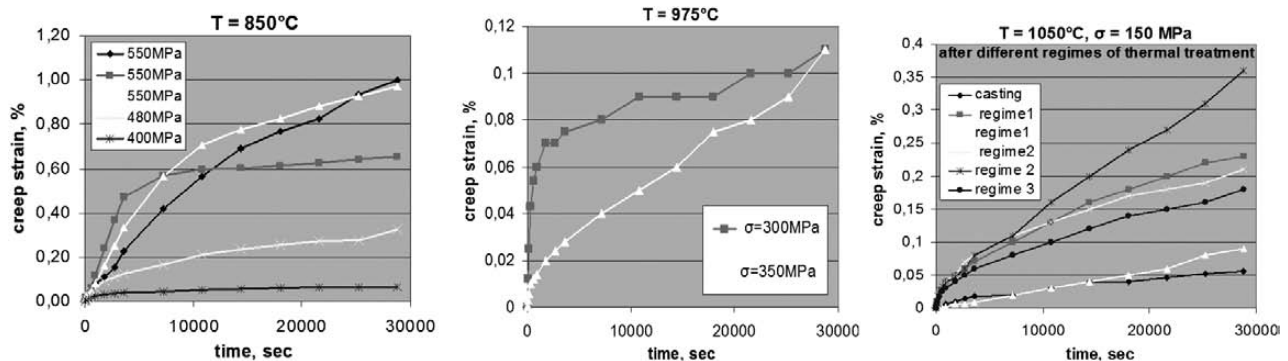


**Figure 2:** Creep curves of alloy ZhS32 at (850, 975 and 1050) °C

**Slika 2:** Krivulje lezenja zlitine ZhS32 pri (850, 975 in 1050) °C

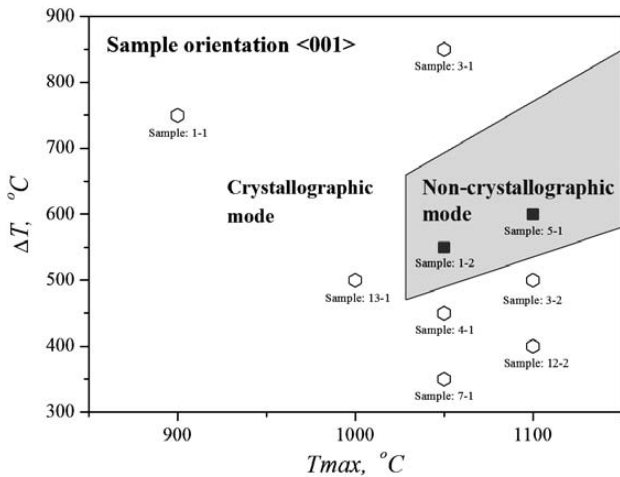


Figure 3: Map of the fracture mechanisms for alloy ZhS32 under thermal cyclic loading

Slika 3: Prikaz področij mehanizmov porušitve za zlitino ZhS32 pri toplotnem cikličnem obremenjevanju

The tests of the ZhS36 alloy show that the conditions for failure under the thermal cyclic loading depend on the crystallographic orientation of the single-crystal alloy and also on the temperatures of the cycle. Unfortunately, the experiments conducted on the ZhS36 alloy with orientations  $\langle 001 \rangle$ ,  $\langle 011 \rangle$  and  $\langle 111 \rangle$  were not numerous and the obtained results reflect only a trend. However, a formulation of the failure criterion depends on the failure mode (crystallographic or non-crystallographic).<sup>6</sup> In this research, we obtained the conditions (a range of thermal-cycle parameters) (Figure 3) for the fracture modes of the ZhS32 alloy with the orientations close to  $\langle 001 \rangle$ . An accumulation of unilateral irreversible deformation (ratcheting) was observed in all the tests (Figure 4) for both alloys.

#### 4 CRITERIA OF FAILURE UNDER STATIC LOADING

Single-crystal superalloys, as a rule, are plastic materials and the possibility of a brittle fracture under static loading of gas-turbine blades is remote. However, this issue requires a special investigation. We considered

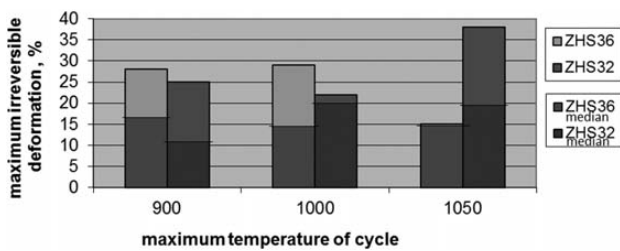


Figure 4: Ratcheting of alloys ZhS32 and ZhS36 under thermal cyclic loading

Slika 4: Zobčenje pri zlitinah ZhS32 in ZhS36 pri toplotnem cikličnem obremenjevanju

such a possibility on the basis of two (stress and deformation) failure criteria.

The effect of stress on deformation capacity  $\epsilon^*$  is determined with the formulas of Mahutov N. A. or Hancock J. W. and Mackenzie A. C.<sup>7</sup>:

$$\epsilon^* = \epsilon_{pr} \cdot 1.7 \exp^{-1.5 \frac{\sigma_{mean}}{\sigma_i}} \quad (1)$$

$$\epsilon^* = \frac{\epsilon_{pr} K_e \sigma_i^2}{3\sigma_1 \sigma_{mean}} \quad (2)$$

where  $\epsilon_{pr}$  is the maximum deformation, determined from the experiments under short-term tension, and  $K_e$  is the characteristic of the material state (in a brittle state  $K_e = 1$ , in a viscous state  $K_e = 1.2$ ).

We need to consider the effect of stress on the fracture conditions in terms of the power criterion. Let us consider the general case of stress:  $\sigma_2 = A_1\sigma_1$ ,  $\sigma_3 = A_2\sigma_1$ , where  $A_1$  and  $A_2$  can vary from  $-\infty$  to 1. Depending on the relations between  $\sigma_1$ ,  $\sigma_2$ ,  $\sigma_3$  and on the ratio of  $\sigma_{pr}/\sigma_{0.2}$ , there is an area of brittle damage, in which the ultimate tensile stress is used as the limiting strength characteristic  $\sigma_{pr}$  for the local stresses.

The above relation can also be written in a different form. Let us consider the case where  $\sigma_1/\sigma_i > 1$ . Using an approximation of the stress-strain curve in the form of  $\sigma_i = \sigma_{0.2} + A\epsilon_i^{p_m}$  and the fracture condition according to the first theory of strength,  $\sigma_1 = \sigma_{pr}$ .  $q = \sigma_1/\sigma_i$ , we obtain  $q(\sigma_{0.2} + A\epsilon_i^{p_m}) = \sigma_{pr}$ , where the plastic deformation is defined with the equation:

$$\epsilon_i^p = \left[ \frac{\sigma_{pr}/q - \sigma_{0.2}}{A} \right]^{\frac{1}{p_m}} \quad (3)$$

For  $k = \sigma_{pr}/\sigma_{0.2}$ , using:

$$\epsilon_i^p = \left[ \frac{\sigma_{pr}k/q - \sigma_{0.2}}{A} \right]^{\frac{1}{p_m}} = \left[ \frac{\sigma_{pr}(k/q - 1)}{A} \right]^{\frac{1}{p_m}}$$

with  $k/q > 1$ , a brittle fracture takes place as  $k/q = 1$ .

An analysis of crack initiation in the blades under static loading (centrifugal force and bending) on the basis of the stress-failure criterion should include:

1. A thermal finite-element analysis of the steady-state temperature field in a blade;
2. An elastic finite-element analysis of the stress fields with the subsequent definitions of  $q = \sigma_1/\sigma_2$  and  $k = \sigma_{pr}/\sigma_{0.2}$  at the corresponding temperatures for all the elements of cooled blades;
3. According to the first strength theory we assume that  $\sigma_{pr} = \sigma_{separation} \approx \sigma_F / (1 - \psi)$  and verify the absence of equality for  $q = k$  at all the points. For the remaining cases, we calculate the values of the plastic strain using equation (3);
4. An estimation of the strength by comparing  $\epsilon_i^p$  (3) with the limiting plasticity  $\epsilon^*$  (1) or (2).

An analysis of the crack initiation in the blades under static loading (centrifugal force and bending) on the basis of the *strain-failure criterion* should include:

1. A thermal finite-element analysis of the steady-state temperature field in a blade;
2. An elastoplastic finite-element analysis with a definition of the zones of plastic deformation and maximum values  $\varepsilon_{i_{max}}^p$  for all the elements of cooled blades;
3. A comparison of the obtained value for  $\varepsilon_{i_{max}}^p$  with the limiting characteristic  $\varepsilon^*$  (1) or (2) at the corresponding temperatures, also taking into account a decrease under the effect of aging at the operating temperatures and during long exposures;
4. A viscoelastic finite-element analysis of the stress-relaxation processes with the initial conditions obtained with the elastoplastic analysis (see 2);
5. A calculation of the equivalent stress. If the value of  $(\sigma_0 - \sigma_{res})/E$  is lower than, or approximately equal to, the maximum ductility under creep conditions at a suitable temperature, determined with the formulas:

$$p^* = \varepsilon_c \cdot 1.7 \exp^{-1.5 \frac{\sigma_{mean}}{\sigma_i}} \quad (4)$$

$$p^* = \frac{\varepsilon_c K_c \sigma_i^2}{3 \sigma_1 \sigma_{mean}} \quad (5)$$

then a brittle fracture under the conditions of stress relaxation is possible.

An acceptance of the assumption that fine micro-cracks are formed in the zone of inelastic deformation. Determination of the size of inelastic deformation (plastic and creep) and a comparison with the limit values corresponding to the beginning of the accelerated crack growth in non-linear fracture mechanics.

### 5 CRITERIA OF FAILURE UNDER THERMAL CYCLIC LOADING

For a prediction of a TMF failure of single-crystal materials, it is reasonable to use the deformation criterion proposed in<sup>6</sup>. The crack-initiation criterion is the condition for achieving the critical value of the total damage initiated by different mechanisms:

$$D_1 (\Delta \varepsilon_{eq}^p) + D_2 (\Delta \varepsilon_{eq}^c) + D_3 (\varepsilon_{eq}^p) + D_4 (\varepsilon_{eq}^c) = 1 \quad (6)$$

The criterion (6) is based on the linear summation of the damages caused by the cyclic plastic strain:

$$D_1 = \frac{1}{C_1} \sum_{i=1}^n (\Delta \varepsilon_{eqi}^p)^k \quad (7)$$

the cyclic creep strain:

$$D_2 = \frac{1}{C_2} \sum_{i=1}^n (\Delta \varepsilon_{eqi}^c)^m \quad (8)$$

the unilaterally accumulated plastic strain:

$$D_3 = \frac{1}{\varepsilon_r^p} \max \varepsilon_{eq}^p \quad (9)$$

and the unilaterally accumulated creep strain:

$$D_4 = \frac{1}{\varepsilon_r^c} \max \varepsilon_{eq}^c \quad (10)$$

$C_1, C_2, k, m, \varepsilon_r^p, \varepsilon_r^c$  are the material parameters depending on the temperature and on the crystallographic orientation. Usually the relations  $k = 2, m = 5/4, C_1 = (\varepsilon_r^p)^k, C_2 = (\frac{3}{4} \varepsilon_r^c)^m$  are used.

Different norms of the strain tensor are considered as an equivalent strain for (6); among them there are: *the maximum shear strain in the slip system* with normal  $\mathbf{n}_{\{111\}}$  to the slip plane and slip direction  $\mathbf{l}_{\{011\}}$ :

$$\varepsilon_{eq} = \mathbf{n}_{\{111\}} \cdot \boldsymbol{\varepsilon} \cdot \mathbf{l}_{\{011\}} \quad (11)$$

*the maximum tensile strain* (the maximum eigenvalue of the strain tensor):

$$\varepsilon_{eq} = \varepsilon_1 = \max \arg \{ \det(\boldsymbol{\varepsilon} - \lambda \mathbf{I}) = 0 \} \quad (12)$$

the von Mises *strain intensity*:

$$\varepsilon_{eq} = \sqrt{\frac{2}{3} \text{dev} \boldsymbol{\varepsilon} \cdot \text{dev} \boldsymbol{\varepsilon}} = \sqrt{\frac{2}{9} [(\varepsilon_x - \varepsilon_y)^2 + (\varepsilon_y - \varepsilon_z)^2 + (\varepsilon_z - \varepsilon_x)^2 + \frac{3}{2} (\gamma_{xy}^2 + \gamma_{yz}^2 + \gamma_{zx}^2)]} \quad (13)$$

and *the maximum shear strain*:

$$\varepsilon_{eq} = \frac{1}{2} [\varepsilon_1 - \varepsilon_3] = \frac{1}{2} [\max \arg \{ \det(\boldsymbol{\varepsilon} - \lambda \mathbf{I}) = 0 \} - \min \arg \{ \det(\boldsymbol{\varepsilon} - \lambda \mathbf{I}) = 0 \}] \quad (14)$$

Equivalent strain (11) corresponds to the crystallographic failure mode, while equivalent strains (12)–(14) correspond to the non-crystallographic failure mode.

### 6 RESULTS OF THE FINITE-ELEMENT SIMULATION

The stress-strain analysis of single-crystal samples (**Figure 1**), with a concentrator (in the form of a central circular hole) or without a concentrator, was carried out on the basis of the finite-element program PANTOCRATOR<sup>8</sup> with an application of physical models of plasticity. These material models take into account that an inelastic deformation occurs in accordance with the crystal-slip systems due to a slip mechanism and, therefore, the deformation is strongly sensitive to the crystallographic orientation. The elastoplastic and viscoelastoplastic material models<sup>9,10</sup> with non-linear kinematic and isotropic hardening, also accounting for the self-hardening of each system and the latent hardening<sup>11</sup> between the slip systems, are used in the finite-element simulations. The application of viscoelastic models leads to unrealistically overestimated levels of the stress.

The obtained results for the inhomogeneous stress, strain and damage fields allow us to find the location of the specimen critical point. The damage field is obtained with criterion (6) on the basis of the analysis of the

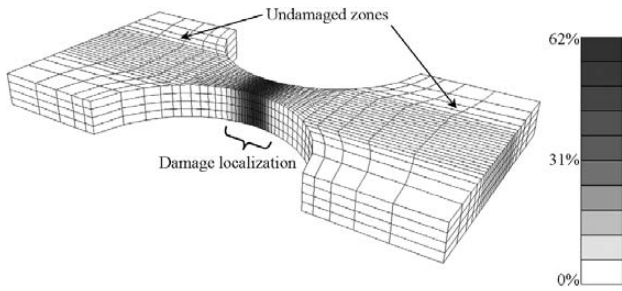


**Figure 5:** Damage-field distribution after the first cycle for sample 5-1 with the  $\langle 001 \rangle$  orientation

**Slika 5:** Širjenje področja poškodbe po prvem ciklu pri vzorcu 5-1 z orientacijo  $\langle 001 \rangle$

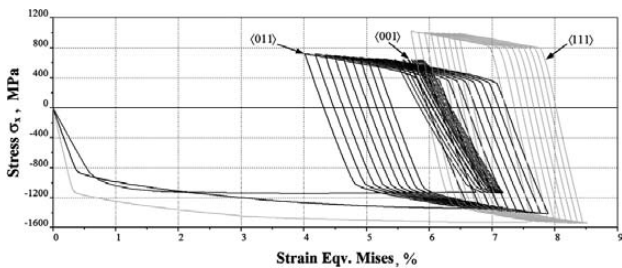


**Figure 6:** Influence of the crystal orientation on the cyclic stress-strain curve. Results of the finite-element simulations of the thermal cycles with  $T_{max} = 900 \text{ }^\circ\text{C}$  and  $T_{min} = 150 \text{ }^\circ\text{C}$  (the central point of the specimen).

**Slika 6:** Vpliv orientacije kristala na ciklično krivuljo napetost – raztezek. Rezultati simulacije s končnimi elementi za toplotne cikle s  $T_{max} = 900 \text{ }^\circ\text{C}$  in  $T_{min} = 150 \text{ }^\circ\text{C}$  (sredinski del vzorca).

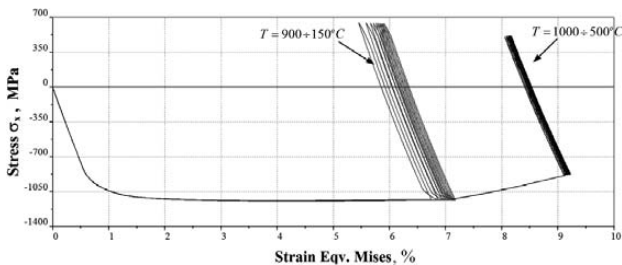


**Figure 7:** Influence of the temperature program on the cyclic stress-strain curve. Results of the finite-element simulations of the specimens with the  $\langle 001 \rangle$  orientation (the central point of a specimen).

**Slika 7:** Vpliv temperaturnega programa na krivuljo napetost – raztezek. Rezultati simulacije s končnimi elementi za vzorce z orientacijo  $\langle 001 \rangle$  (sredinski del vzorca).

strain-field evolution using the experimental data on the creep and elastoplastic deformation-resistance curves. The typical damage-field distribution after the first thermal cycle ( $20 \text{ }^\circ\text{C} \rightarrow T_{max} = 900 \text{ }^\circ\text{C} \rightarrow T_{min} = 150 \text{ }^\circ\text{C}$ ) is presented in **Figure 5** for sample 5-1 of ZhS36 with orientation  $\langle 001 \rangle$ .

The results of the finite-element simulations show that the crystallographic orientation has a significant influence on the stress-strain state of the samples (**Figure 6**), as confirmed also by the experiments.<sup>12</sup> The width of the hysteresis loops and the unilaterally accumulated strain are also very sensitive to the thermal cyclic regime (**Figure 7**).

The numbers of the cycles to crack initiation, calculated on the basis of criterion (6) using different equivalent strains, (11)–(14), are given in **Table 3**. A satisfactory correlation is observed between the criterion predictions and the results of the experiments (without a sufficient statistical representation).

## 7 CONCLUSIONS

1. In the investigations of I. L. Svetlov, E. R. Golubovsky and other researchers a series of tests were conducted regarding the definition of the thermal fatigue resistance and short-term creep of the single-crystal ZhS32 alloy, determining the temperature range causing the changes in the failure modes.
2. The failure criteria for the single-crystal alloys under static and thermal cyclic loadings are proposed and discussed. A satisfactory correlation is observed between deformation criterion (6) and the obtained experimental results. All the considered variants of equivalent strains (11)–(14) give practically the same results. The criterion using von Mises strain intensity (13) offers the most conservative estimation.
3. The finite-element simulations of single-crystal specimens under thermal cyclic loading were performed using different material models. The obtained results indicate an applicability of the proposed deformation criteria of failure for the single-crystal ZhS32 and ZhS36 alloys for the temperatures up to  $1100 \text{ }^\circ\text{C}$ .

**Table 3:** Deformation-criterion (6) predictions vs. experimental results for the crack initiation life

**Tabela 3:** Napovedi merila deformacij (6) v odvisnosti od eksperimentalnih rezultatov za začetek nastanka razpoke

	Orientation	$T_{max}/^\circ\text{C}$	$T_{min}/^\circ\text{C}$	Number of cycles to crack initiation				Experiment
				$\epsilon_{eq} = \epsilon_{nl}$ (11)	$\epsilon_{eq} = \epsilon_1$ (12)	$\epsilon_{eq} = \epsilon_i$ (13)	$\epsilon_{eq} = \gamma_{max}$ (14)	
Sample 5-1		900	150	338	275	195	280	435
Sample 5-3		1000	500	218	196	150	172	305
Sample 1-2		900	150	85	73	59	75	190
Sample 2-1		900	150	15	9	10	15	17
Sample 1-1*		900	150	5	4	3	4	10
Sample 2-6*		1000	500	61	44	56	57	10–130
Sample 4-1*		900	150	6	4	4	5	10

\*Specimen with a concentrator (the radius of the central hole is 0.25 mm)

## Acknowledgements

The study was supported by the Russian Fundamental Research Program, Project No.12-08-00943. The authors are also grateful to S. M. Odabai-Fard for helping prepare the paper.

## 8 REFERENCES

- <sup>1</sup>E. N. Kablov, E. R. Golubovsky, Heat-resistant nickel alloys, Mechanical Engineering, Moscow 1998
- <sup>2</sup>R. E. Shalin, I. L. Svetlov, E. B. Kachanov, V. N. Toloraiya, O. S. Gavrilin, Single crystals of nickel-base superalloys, Mechanical Engineering, Moscow 1997
- <sup>3</sup>L. B. Getsov, N. I. Dobina, A. I. Rybnikov, A. S. Semenov, A. A. Staroselsky, N. V. Tumanov, Thermal fatigue resistance of single crystal alloy, Strength of Materials, (2008) 5, 54–71
- <sup>4</sup>L. B. Getsov, A. I. Rybnikov, A. S. Semenov, Thermal fatigue strength of heat-resistant alloys, Thermal Engineering, 56 (2009), 412–420
- <sup>5</sup>L. B. Getsov, Materials and strength components of gas turbines, Rybinsk, Publ. House, Gas Turbine Technology, 1–2 (2011)
- <sup>6</sup>L. B. Getsov, A. S. Semenov, Failure criteria for polycrystalline and single crystal materials under thermal cyclic loading, Proc. NPO CKTI, N296, Strength of materials and resource elements of power, St. Petersburg, 2009, 83–91
- <sup>7</sup>L. B. Getsov, B. Z. Margolin, D. G. Fedorchenko, The determination of elements of engineering safety margins in the calculation of structures by finite element method, Proc. NPO CKTI, N296, Strength of materials and resource elements of power, St. Petersburg, 2009, 51–66
- <sup>8</sup>A. S. Semenov, PANTOCRATOR-finite-element software package, focused on the solution of nonlinear problems in mechanics, Proc. of V Int. Conf. Scientific and technical problems of forecasting the reliability and durability of the structures and methods for their solution, Publishing House of Polytechnic University, St. Petersburg 2003, 466–480
- <sup>9</sup>G. Cailletaud, A Micromechanical Approach to Inelastic Behaviour of Metals, Int. J. Plast., 8 (1991), 55–73
- <sup>10</sup>J. Besson, G. Cailletaud, J. L. Chaboche, S. Forest, Non-linear mechanics of materials, Springer, 2010
- <sup>11</sup>U. F. Kocks, T. J. Brown, Latent hardening in aluminium, Acta Metall., 14 (1966), 87–98
- <sup>12</sup>L. Getsov, A. Semenov, A. Staroselsky, A failure criterion for single crystal superalloys during thermocyclic loading, Mater. Tehnol., 42 (2008) 1, 3–12